

Intermittent Turbulence In the Attachment Line Flow Formed On An Infinite Swept Wing

Ian Poll
University of Manchester
Dept. of Engineering
Manchester, England M139PL

Abstract

The transition process which takes place in the attachment-line boundary layer in the presence of gross contamination is an issue of considerable interest to wing designers. It is well known that this flow is very sensitive to the presence of isolated roughness and that transition can be initiated at a very low value of the local momentum thickness Reynolds number. Moreover, once the attachment line is turbulent, the flow over the whole wing chord - top and bottom surface - will be turbulent and this has major implications for wing drag.

In order to investigate this phenomenon and produce a quantitative model of the development of intermittent turbulence with both Reynolds number and spanwise position, tests have been performed on a series of geometrically similar cylinder models. Data has been gathered on different sized models, in different low-speed wind-tunnels over a wide range of sweep angles (20° to 70°). A model of the transition process has been produced using Emmons' sport theory and the data have been used to determine the models' various unknown constants. Brief consideration is also given to the effects of high speed compressibility and heat transfer. The model provides a good description of the process over a very wide range of conditions.

Intermittent and Low Reynolds Number Turbulence In the Attachment Line Flow Formed On An Infinite Swept Wing

Ian Poll

University of Manchester

Dept. of Engineering

Manchester, England M13 9PL

The work which I presented related to the transition process which can occur on the leading edge of an infinite swept wing i.e. one in which the surface pressure field has no spanwise variation. To be more specific the transition which can occur in the attachment-line boundary layer. This is the boundary layer which forms on the line which divides the upper surface flow from the lower surface flow - see figure 1. The present study relates to two aspects of this problem.

- a) The spanwise development of intermittent turbulence downstream of a large 2-D trip
- and
- b) The relaminarisation of the fully developed turbulent flow as the value of the characteristic Reynolds number, \bar{R} (see figure 2) is progressively reduced.

Since item a) is a classic example of a by-pass transition process, the work is primarily experimental. However, the experiment is not easy for the following reasons.

- 1. The attachment line transition is a "high Reynolds number" phenomenon. There is no way that it can be investigated with bench top scale experiments. The achievement of the necessary conditions requires the use of large models in industrial scale wind tunnels. This makes the problem difficult to study in University laboratories. However at Manchester we are fortunate in having a large scale low speed wind tunnel (9' x 7' test section, maximum speed 250 ft/sec) which is suitable for the study.
- and
- 2. Even with the necessary facilities the attachment line boundary layers are very thin with the turbulent flows being less than 5 mm thick. When this is coupled with the problem of the model being a large distance (2' to 3') from the tunnel wall or floor, it is apparent that conventional traversing of the boundary layer is impossible. Therefore, we have developed a novel and simple approach involving the use of a range of impact pressure probes mounted on the model at a fixed height above the surface. By measuring the indicated pressure over a wide range of tunnel speed, model leading-edge sweep-angle, probe size and probe spanwise location, it is possible to generate a matrix of data which can be interpolated to produce conventional velocity profile information with very high levels of accuracy.

Figures 1 to 16 describe in sequence the way in which the problem of describing the attachment line transition. By combining the data with a model developed from Emmons spot hypothesis an accurate, quantitative description of the process has been produced. A particularly interesting conclusion from this study has been that, whilst an infinite swept (spanwise invariant) laminar and fully turbulent attachment line boundary layers can be set up, the transitional case always exhibits spanwise variation - there is no physically realisable, spanwise invariant, transitional, attachment-line flow!

Figures 17 to 25 summarise our contribution to item b) - the relaminarisation of the fully turbulent attachment line boundary layer by reducing the characteristic Reynolds number. All the information shown corresponds to flows which are fully turbulent. This means that, if a hot wire anemometer is placed in the flow, the signal will be turbulent (no laminar gaps) the whole time. Nevertheless it is clear that the flow does not have the structure of a high Reynolds number turbulent boundary layer.

It is apparent from the velocity profiles that, at the highest Reynolds number conditions, the inner region of the boundary layer obeys the "universal law of the wall". However as the Reynolds number (\bar{R}) is reduced below 600, the profiles are shifting relative to the universal law in a way which is consistent with a Reynolds number variation in the additive constant (c). The shift in the inner region is monotonic with \bar{R} and, at the lowest Reynolds number, the value of the additive constant is about 7.5 compared with 5.2 at large Reynolds number. By computing the velocity profile with a full field boundary layer code, it has been found that the observed changes in the profile are consistent with the following turbulence mode.

1. Von Karman's constant invariant at 0.41.
2. Van Driest's damping factor (A^+) rising rapidly as the Reynolds number falls.
- and 3. The outer mixing length (Lo/δ) rising slowly with decreasing Reynolds number.

We have also observed that as the Reynolds number drops the shape factor H rises very rapidly, achieving a value of about 2 and that the skin friction coefficient goes through a maximum - all this occurring whilst the flow is still "fully turbulent".

Many (if not all) of these features have been observed in low Reynolds number pipe and channel flow. However, they have not been observed in 2-D flat plate, zero pressure gradient flow. This is because, at the Reynolds number which need to be achieved, flat plate flow is invariably contaminated by the disturbances introduced by the trip (needed to make the flow turbulent). Different tripping devices produce different flow fields at these conditions and the underlying behaviour of the turbulence cannot be separated out.

The most important conclusion of the work to date is that relaminarisation can be modelled by an appropriate variation A^+ .

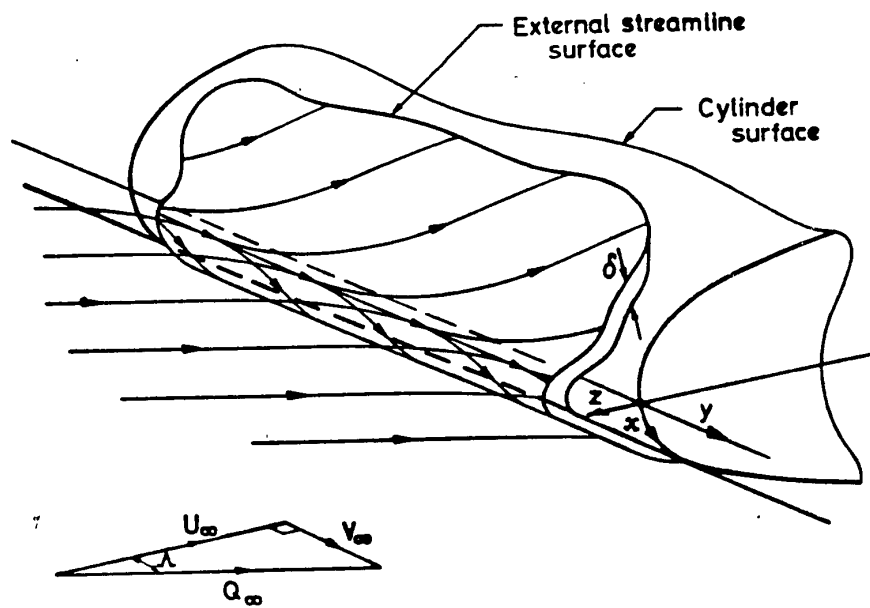


Fig. 1. Flow near the leading edge of a swept cylinder.

INFINITE SWEPT ATTACHMENT LINE PARAMETERS

$$\text{LENGTH SCALE } \gamma = \left\{ \frac{\nu_e}{(\frac{du_e}{dx})_{x=0}} \right\}^{1/2}$$

$$\text{REYNOLDS NUMBER } \overline{R} = \frac{V_e \gamma}{\nu_e}$$

TRIP - DETECTOR SEPARATION = s

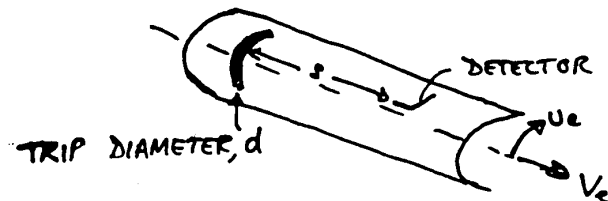


Figure 2

(3)

INTERMITTENCY DEFINED AS A WEIGHTING FUNCTION

$$\text{SKIN FRICTION} \quad Cf = \gamma_1 (C_f)_T + (1-\gamma_1) (C_f)_L$$

$$\text{HEAT TRANSFER} \quad St = \gamma_2 (St)_T + (1-\gamma_2) (St)_L$$

$$\text{LOCAL DYNAMIC PRESSURE} \quad \frac{1}{2} \rho V^2 = \gamma_3 \left(\frac{1}{2} \rho V^2 \right)_T + (1-\gamma_3) \left(\frac{1}{2} \rho V^2 \right)_L$$

etc.

$$\text{IN GENERAL} \quad \gamma_3 = \gamma_3(z)$$

$$\text{BUT AS } z \rightarrow 0 \quad \gamma_3 \rightarrow \gamma_2 \approx \gamma_1 = \gamma$$

Figure 5

(4)

POLL (1983) PROPOSED, ON THE BASIS OF AN EXTREMELY LIMITED AMOUNT OF DATA, THAT FOR CONSTANT S

$$\gamma = 1 - \exp \left[-0.411 \left(\frac{\bar{R} - \bar{R}_B}{\lambda} \right)^2 \right]$$

WHERE \bar{R}_B IS THE VALUE APPROPRIATE FOR THE ONSET OF TRANSITION AND

$$\lambda = \bar{R}_{\gamma=0.75} - \bar{R}_{\gamma=0.25}$$

$$\begin{aligned} \lambda &= \lambda(\bar{R}_B, s/\eta_B) \quad \text{NOT KNOWN} \\ \bar{R}_B &= \bar{R}_B(s/\eta, d/\eta) \quad \text{KNOWN} \end{aligned}$$

Figure 6

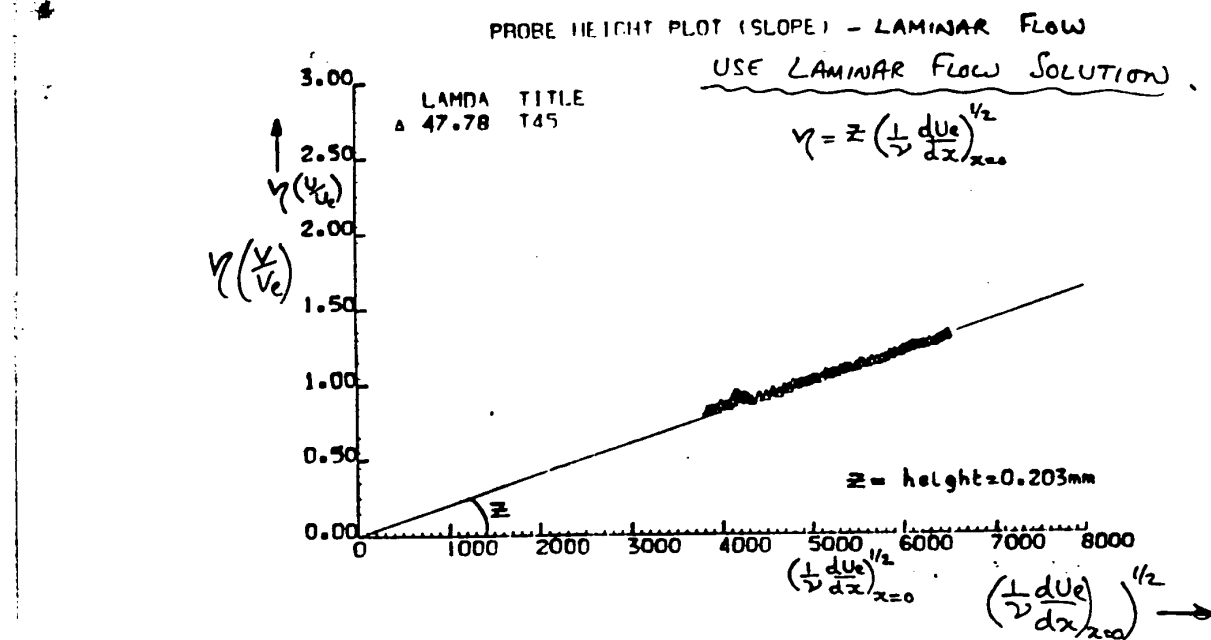


Figure 9

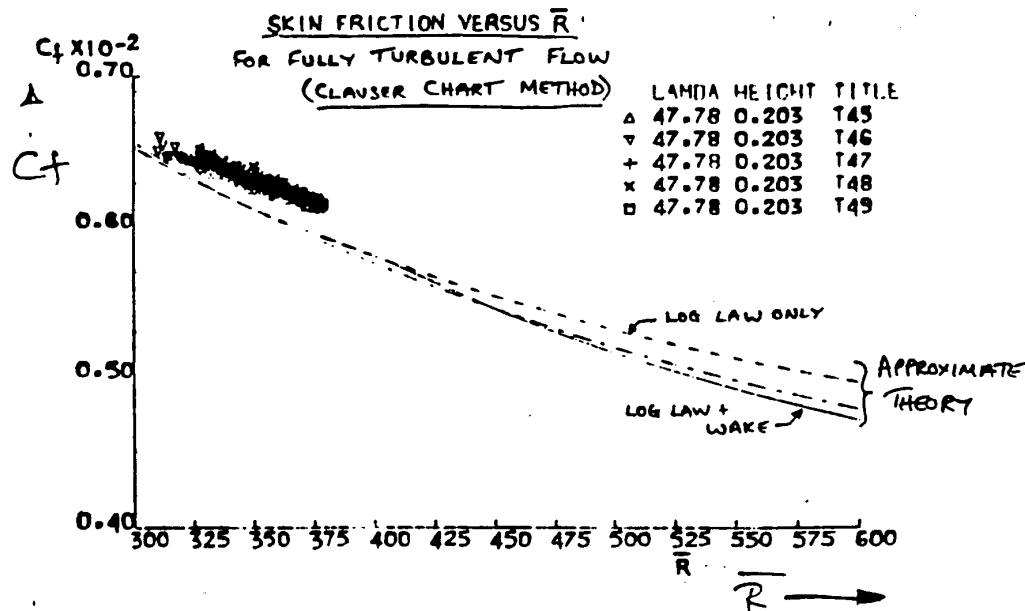


Figure 10

LINEARISED INTERMITTENCY PLOT

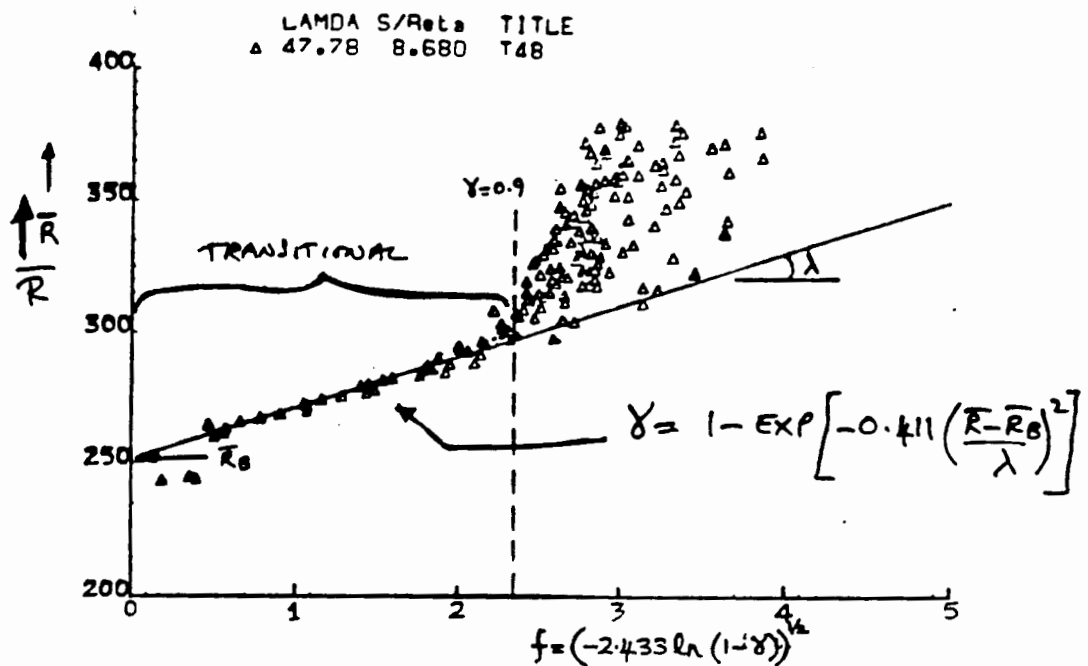
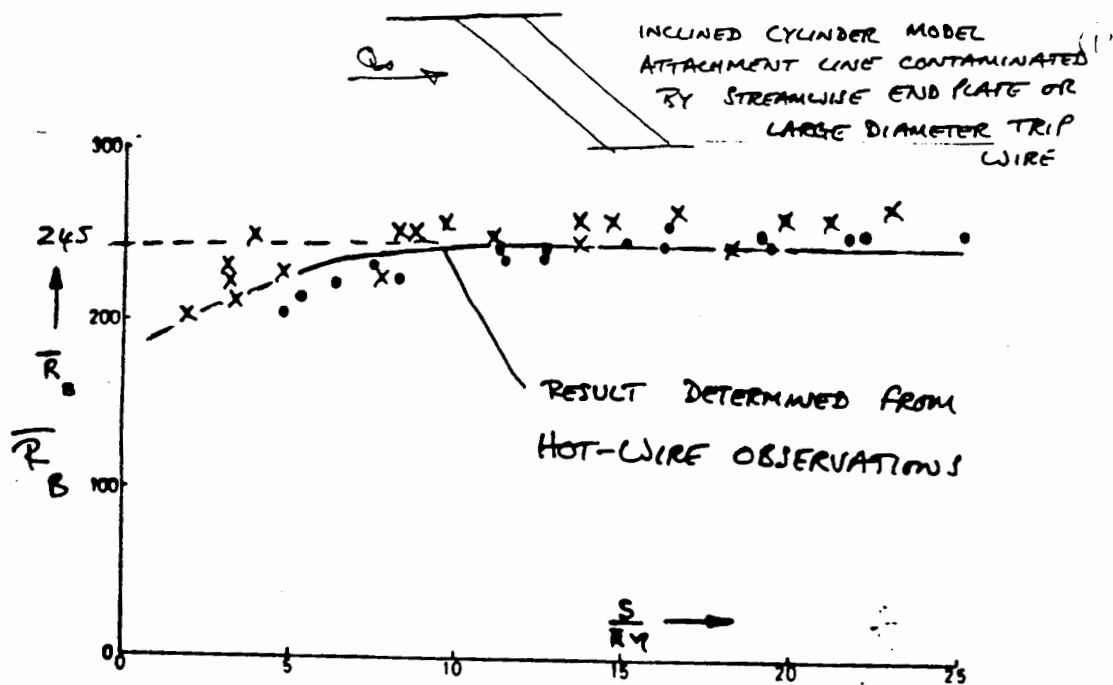


Figure 13



VARIATION OF \bar{R} WITH $S(\bar{R}_B)$ FOR THE ONSET OF TRANSITION

Figure 14

VELOCITY PROFILES FOR VARIOUS RBAR
DANKS DATA

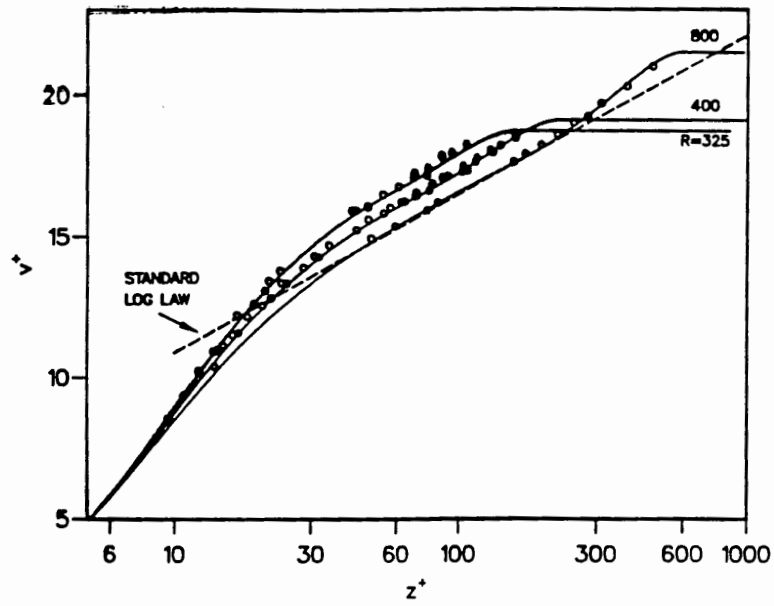


Figure 17

VELOCITY PROFILES FOR VARIOUS RBAR
CUMPSTY'S DATA

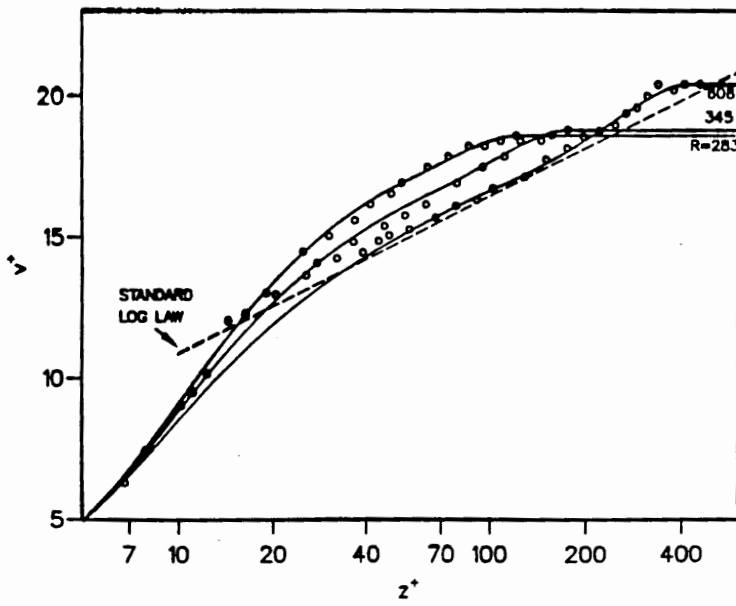


Figure 18

RTHETA VERSUS RBAR

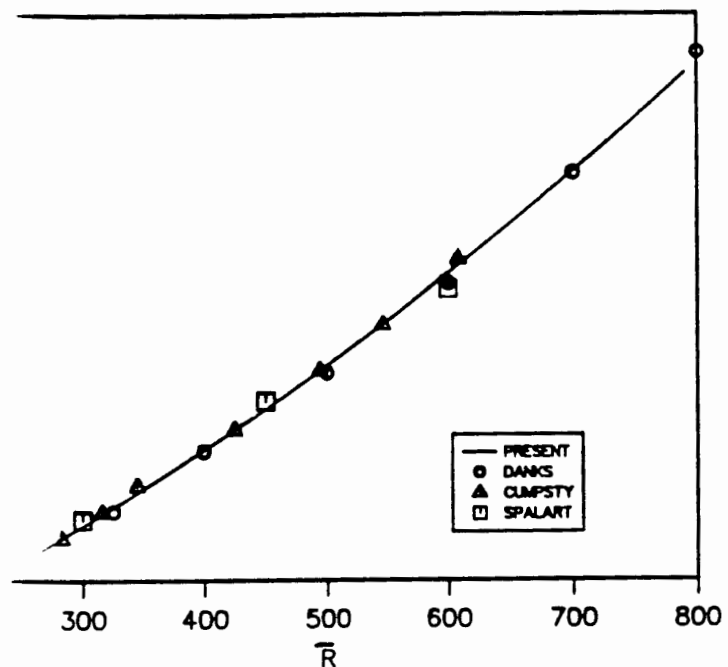


Figure 21

DRIEST DAMPING FACTOR VERSUS DELTA+

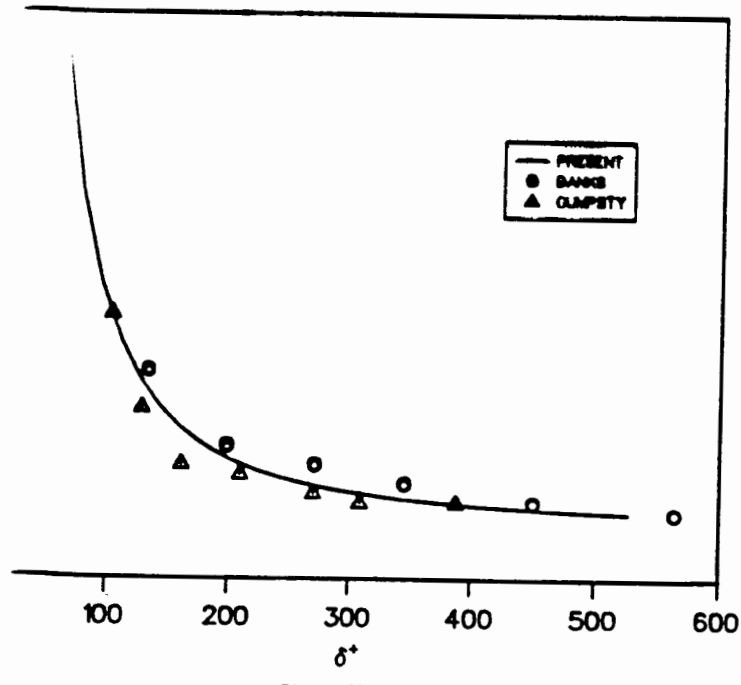


Figure 22

WAKE STRENGTH VERSUS DELTA+

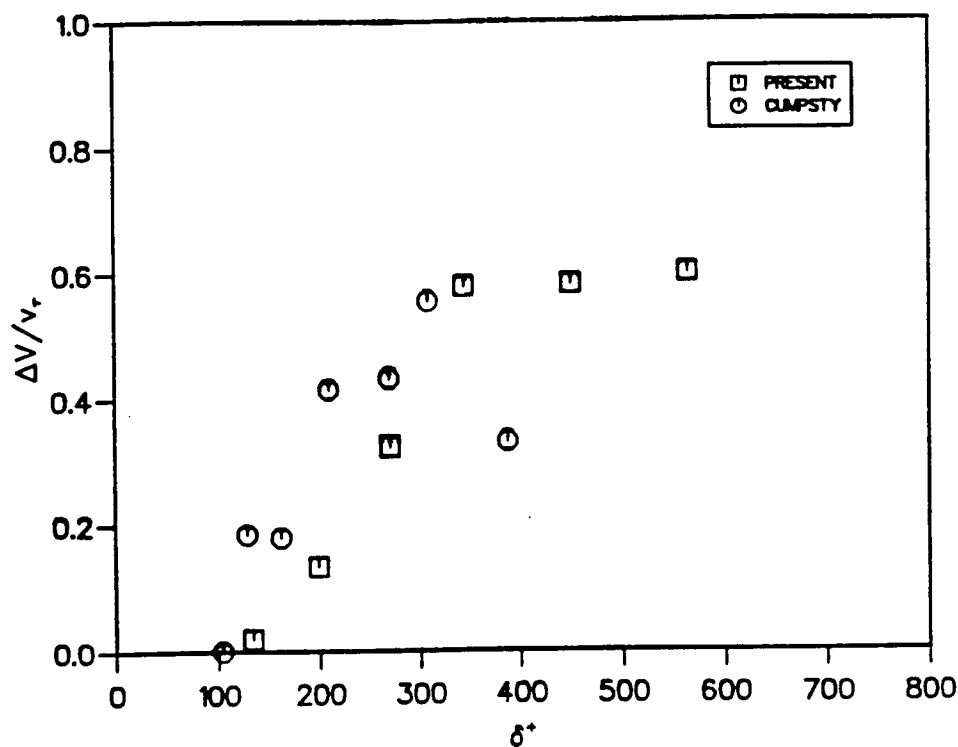


Figure 25

